Journal of Physiology (1989), **414**, *pp.* 201–222
With 9 text-figures
Printed in Great Britain

IDENTIFICATION OF IONIC CURRENTS AT PRESYNAPTIC NERVE ENDINGS OF THE LIZARD

BY CLARK A. LINDGREN AND JOHN W. MOORE

From the Department of Neurobiology, Duke University Medical Center, Durham, NC 27710, USA

(*Received 16 August 1988*)

SUMMARY

1. Ionic currents associated with the invasion of an action potential into the motor nerve ending of the lizard, *Anolis carolinensis*, were measured with a focal extracellular electrode at several locations along the nerve ending.

2. These experimentally observed currents could be matched with computer simulations of action potential propagation into the nerve ending. They revealed that while Na^+ channels are the major ionic current pathway in the heminode, K^+ channels provide the major pathway in the terminal branches and boutons.

3. Calcium current in the presynaptic ending was unmasked by the application of tetraethylammonium (TEA). This current was blocked by: (a) cadmium, (b) ω-conotoxin GVIA and (c) nifedipine, but was unaffected by nickel at concentrations less than or equal to 100 μM. Nifedipine's action became more definitive when the duration of the action potential was greatly extended by pre-treatment with TEA. The effect of Bay K 8644 was inconsistent.

4. Transmitter release, as measured by postsynaptic current, had a pharmacological response profile similar to that of the Ca^{2+} current, with the exception that transmitter release was increased reliably and reversibly by Bay K 8644.

5. This pharmacological response profile is identical to that of the L type Ca^{2+} channel identified by Fox, Nowycky & Tsien (1987*a*) in chick dorsal root ganglion neurones. We saw no evidence for more than a single type of Ca^{2+} channel in lizard motor nerve endings.

6. A calcium-activated K^+ current $I_{K(Ca)}$ was revealed by application of 3,4-diaminopyridine (DAP), a delayed-rectifier K^+ channel blocker. This K(Ca) current was blocked by TEA, charybdotoxin and by substitution of cobalt for extracellular calcium.

INTRODUCTION

The use of focal extracellular electrodes for measurement and identification of localized ionic currents in a nerve ending was first demonstrated by Katz & Miledi (1965) at the neuromuscular junction of the frog. Mallart and collaborators (Brigant & Mallart, 1982; Mallart, 1985) extended this technique to identify a Na^+, Ca^{2+}, and

two types of K^+ current in motor nerve endings of the mouse. We have found the neuromuscular junction on the flat and thin ceratomandibularis muscle in the lizard to be particularly well suited to this approach and have used this preparation to extend our understanding of the ionic conductances in the presynaptic nerve ending and the relationship of these to neurotransmitter release.

We have demonstrated that motor nerve endings in the lizard, as in the mouse, contain four separate conductances: Na^+, K^+, Ca^{2+} and Ca^{2+}-activated K^+(K(Ca)). Furthermore, by incorporating these conductances into a computer model of the nerve ending, we have been able to simulate the current patterns recorded from the nerve endings and assign relative densities of the various channel types throughout the ending.

The observation of multiple Ca^{2+} channel types in a single neurone raises the question as to the role of each and in particular, which type is most closely correlated with transmitter release (see Discussion). The observation that these Ca^{2+} channel types have different sensitivities to pharmacological agonists and antagonists (Fox *et al.* 1987*a*) has allowed us to identify the Ca^{2+} channel type present at the lizard neuromuscular junction. We found that (a) the dihydropyridine-sensitive channel ('L' in the nomenclature of Fox *et al.* 1987*a*) is the major Ca^{2+} channel type in the motor nerve ending of the lizard and (b) alterations of its magnitude cause corresponding changes in transmitter release. Some of the results reported here have appeared in preliminary form (Lindgren & Moore, 1986; Lindgren & Moore, 1987; Lindgren, Moore & Sostman, 1988).

METHODS

Preparation

Approximately 80% of the fibres in the ceratomandibularis muscle of the lizard, *Anolis carolinensis*, have the single *en plaque* innervation characteristic of the twitch muscle fibre type described in the scalenus (Proske & Vaughan, 1968) and intercostal muscles of the lizard (Walrond & Reese, 1985). In contrast to the extensive neuromuscular junction of the frog, which extends 150–200 μm, the motor endings of lizard twitch fibres are compact, extending only 30–60 μm (Walrond & Reese, 1985). They are composed of fairly large boutons, approximately 5–10 μm in diameter, which are connected by short, tubular segments of unmyelinated axon, approximately 1–2 μm in diameter.

The remainder (approximately 20%) of the fibres in the ceratomandibularis muscle are innervated by nerve endings consisting of smaller boutons, 2–5 μm in diameter, connected by very fine segments of axon, less than 1 μm in diameter. These fibres are morphologically similar to the fast twitch fibres described in mammalian extensor digitorum longus fibres (Ellisman, Rash, Staehelin & Porter, 1976) as well as lizard intercostal muscle (John Walrond, personal communication). We found no obvious differences in the electrical properties of these two types of endings and thus used data from both types interchangeably.

Dissection and solutions

Small (5–8 cm) lizards, *Anolis carolinensis*, were obtained from Carolina Biological Supply Company (Burlington, NC, USA). Prior to experimentation, they were decerebrated either by destroying the brain with a pithing needle or by removing the top of the head with a single cut across the upper jaw, caudal to the eyes (Proske & Vaughan, 1968; Barrett & Barrett, 1982; Walrond & Reese, 1985; Barrett, Morita & Scappaticci, 1988). To minimize unnecessary discomfort, the lizards were placed in a container at 5 °C for at least 10 min prior to decerebration.

The cold anaesthesia was verified by the absence of the tail prick or corneal reflexes. The ceratomandibularis muscle and its motor nerve, a small branch of the hypoglossal nerve, were then dissected from the lower jaw and perfused with saline of the following composition (in mM): NaCl, 130; KCl, 3; $NaHCO_3$, 20; $CaCl_2$, 2; glucose, 5 (Proske & Vaughan, 1968). Co^{2+}, Ni^{2+} and Cd^{2+} were added as chloride salts. The saline was gassed with a 95–5% mixture of O_2 and CO_2, which maintained the pH at 7·2. The temperature was maintained ($\pm 0{\cdot}1$ °C) with a thermoelectric cooling device at a chosen value between 15·0 and 25·0 °C.

Tetraethylammonium bromide (TEA), 3,4-diaminopyridine (DAP) and nifedipine were obtained from Sigma Chemical Company. ω-Conotoxin GVIA was purchased from two different sources, Peninsula Laboratories (Belmont, CA, USA) and American International Chemicals (Natick, MA, USA). The Bay K 8644 was kindly provided by Dr Alexander Scriabine (Miles Laboratories) and the charybdotoxin (CTX) was provided and purified (to approximately 40% purity) by Dr Chris Miller (Brandeis University).

Elimination of postsynaptic current

Whereas transmitter release was estimated on several occasions by measuring the amplitude of the postsynaptic current, this current was generally eliminated when measuring the much smaller presynaptic currents (to avoid possible distortions and interference). We were surprised to find that the postsynaptic current was only partially blocked by tubocurarine chloride at a concentration of 50 μM. For comparison, Brigant & Mallart (1982) used 20–100 μM-tubocurarine to completely block the acetylcholine (ACh) receptors at the mouse neuromuscular junction. Although curare was only partially effective in the lizard, complete block of the postsynaptic current was obtained by bath application of the curariform drug, pancuronium bromide, at a concentration of only 5 μM.

Electrode positioning and current measurement

This preparation is so thin that the nerve endings and the heat-polished tip (inside diameter approximately 5 μm) of the electrode can be viewed under high power (640 ×) Nomarski optics in a Zeiss inverted microscope. The electrode (1·2 mm glass; World Precision Instruments, New Haven, CT, USA) was filled with standard saline and had a resistance of about 1 MΩ. It could be readily and reversibly (i.e. the signals observed were reproducible) placed against the heminode or terminal branches. Usually the tip of the electrode became mechanically 'stuck' to the underlying membrane and/or connective tissue sheath, allowing for prolonged and stable recording. However, the resistance of the seal was only about 100–200 KΩ, not in the range of gigaohms normally attained in patch clamp recording.

Currents were measured and filtered by a conventional patch clamp amplifier (Axopatch, Axon Instruments, Burlingame, CA, USA). The signals were digitized by a 12 bit analog-to-digital converter (Data Translation 2818) and stored on discs in an IBM PC-XT computer for averaging, analysis and plotting. To improve the signal-to-noise ratio, 25 to 100 current signals were averaged and, when necessary, further smoothed by passing the average signal through a three or five point digital time–domain filter. The equations are:

$$\text{3-point, } Y_i = 0{\cdot}25\,Y_{i-1} + 0{\cdot}5\,Y_i + 0{\cdot}25\,Y_{i+1}; \tag{1}$$

$$\text{5-point, } Y_i = 0{\cdot}1\,Y_{i-2} + 0{\cdot}2\,Y_{i-1} + 0{\cdot}4\,Y_i + 0{\cdot}2\,Y_{i+1} + 0{\cdot}1\,Y_{i+2}. \tag{2}$$

In all cases where we observed significant variability in our experimental findings, this is stated explicitly in the text and the experiment most representative of the results was chosen for presentation. In all other cases, the reported experimental results were uniform and were observed at least three times.

Because the tip of the electrode has relatively thick glass walls and dimensions on the order of the nerve terminal boutons, one might expect distortion of the current patterns when the amplifier is used in the current-to-voltage conversion mode. But since the shape of the wave forms did not change when the amplifier was switched to the voltage-follower mode (that is, when no current was drawn through the electrode), we know that the electrode itself does not significantly affect the signal. These results are consistent with the observation that the electrode resistance is approximately tenfold higher than the seal resistance, so that only about 10% of the membrane current actually passes through the electrode.

Simulations of presynaptic currents

Computer simulations of the propagation of a nerve impulse into the nerve ending were carried out on an IBM PC-AT or Compaq Deskpro-386 using a program written in C-language to solve cable-equations. (This program, CABLE, is described in much greater detail in Hines (1989) and is available from Dr Michael Hines, Department of Neurobiology, Duke University Medical Center, Durham, NC 27710, USA). Briefly, the simulations were based on standard nerve cable equations (Hodgkin, 1937) which utilized expressions for Na^+, K^+ and leakage conductances as described by Hodgkin & Huxley (1952). Specific geometrical and electrical properties were assigned to the CABLE program by calls made from another program written in Focal, a convenient and simple interpretive language.

We used electron microscopic data (Walrond & Reese, 1985) and our own observations made at the light microscope level to describe the morphology of the lizard neuromuscular junction. To provide a realistic electrical source (voltage and impedance) for the ending, the simulations included three proximal nodes with internodal spacing decreasing from 200 to 50 μm between the last node and the heminode (see Discussion). The ending was simulated as a short heminode region (4 μm $\times$ 4 μm), followed by three identical branches with four boutons each, separated by short intervening axons (see Fig. 1*B* and Table 1).

Criteria of fit of simulations to data

To be included in our data set, we required that the simulations satisfy the following criteria: (1) they must match the normally observed current patterns at five different loci in the nerve ending as shown in Fig. 1, (2) they must match the patterns at the heminode and bouton 2 in the presence of TEA (Fig. 4) and (3) they must match the patterns at the heminode and bouton 2 in the presence of TEA and cobalt (data not shown).

RESULTS

Spatial distribution of ionic currents

Experimental results

Ionic currents resulting from the invasion of an action potential into the nerve ending were recorded at different locations, as shown in Fig. 1*A*, by carefully positioning the heat-polished tip (approximately 5 μm i.d.) of an extracellular electrode. The current flow is predominantly inward at the transition between the myelinated and non-myelinated portions of the axon (record *e*, Fig. 1*A*). This region is called a 'heminode' because it is anatomically equivalent to one-half of a node of Ranvier. Over the remainder of the ending the predominant net current flow is outward (records *a–d*, Fig. 1*A*). Brigant & Mallart (1982) interpreted similar current patterns which they observed at motor nerve endings of the mouse by arguing that Na^+ current dominates in the heminode and K^+ current dominates in the terminal branches and boutons. Pharmacological identification of the various current components performed in parallel with computer simulations have led us to similar conclusions for lizard motor endings.

As can be seen in Fig. 1*A*, the current in the heminode region (record *e*) contains an initial, brief outward (positive) phase, followed by two inward (negative) peaks. The initial positive current is that which discharges the membrane capacitance as the action potential invades the ending. The first of the two negative peaks represents active Na^+ current influx in the heminode, and the second a Na^+ return path (or 'sink') for the efflux of K^+ in the distal part of the terminal. Over the remainder of

the ending (records *a–d*, Fig. 1*A*) the net current flow is outward in the form of two peaks. These peaks represent the discharging of the membrane capacitance by the passive spread of current into the terminal branches, followed by the outward delayed K^+ current generated in the distal terminal membrane.

Simulations

We simulated these current patterns on a computer, assigning channel densities which would allow us to match our experimental records. These simulations showed that if the internodal spacing is progressively decreased along the motor axon from

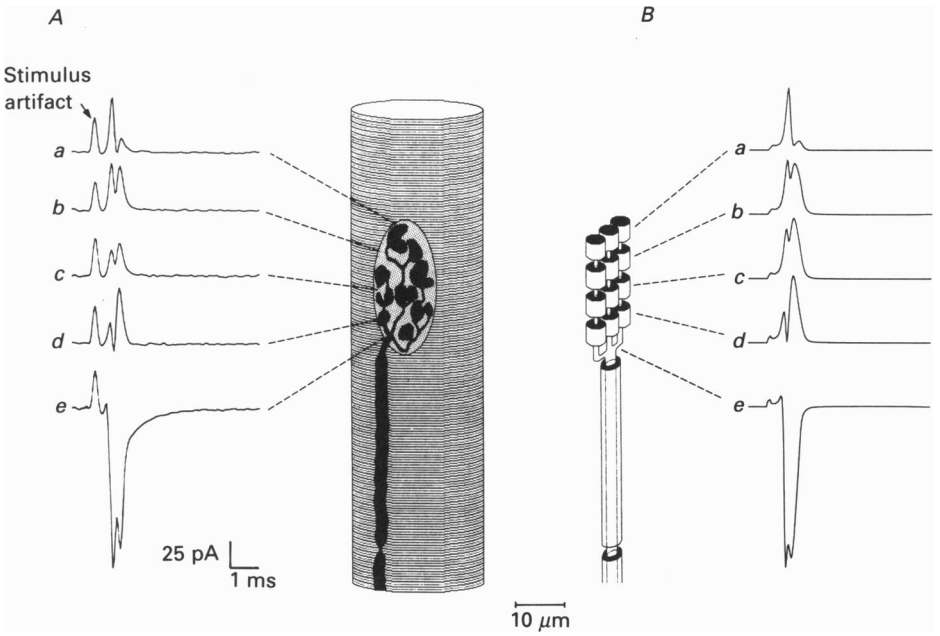

Fig. 1. Current patterns at the distal terminal (*a–d*) and heminode (*e*) in motor nerve endings of the lizard. *A*, current was measured with an extracellular electrode at the five positions (*a–e*) indicated on the drawing of a lizard neuromuscular junction. Downward peaks correspond to inward current. Postsynaptic current was blocked completely with 10 μM-pancuronium bromide. Temperature 20 °C. Each pattern is the average of 100 traces obtained at a stimulation rate of 0·5 Hz. *B*, simulated patterns of membrane current at the heminode and four boutons. Parameters and geometry are given in Table 1.

the normal 1–2 mm distance down to about 50 μm as the neuromuscular junction is approached (see Quick, Kennedy & Donaldson, 1979), then the nerve impulse will propagate easily into the nerve ending without requiring Na^+ channels in the terminal membrane.

The simulated currents were generated by Na^+, K^+ and leakage conductances as described by Hodgkin & Huxley (1952). Ionic channel densities were tentatively assigned to the various components of the nerve ending from our interpretations of the extracellular focal current records. We assumed that Na^+ channels dominated in the nodes and heminode but that K^+ channels dominated in the distal terminal, with

a region of relatively smooth crossover intervening. This assignment of channel densities was then varied over a wide range of parameter space in an effort to match our experimental data set (see Methods: Criteria of fit of simulations to data). Our simulation of the normal current patterns observed at five locations in the ending is shown in Fig. 1*B*.

The nodes were assigned a tenfold higher density of Na^+ channels than that for Hodgkin–Huxley squid axons, as is usually assumed in simulations of propagation in myelinated fibers (for a review, see Moore, Joyner, Brill & Waxman, 1977). Beginning with the heminode, the Na^+ channel density was reduced rapidly, and in the final bouton it was a small fraction of that in the node. The K^+ channel density assigned to the nodes was about 1% of that usually assigned to frog nodes, but was progressively increased in the heminode and boutons up to approximately that in frog nodes. The leakage conductance was quite low throughout the nerve ending (2% of that used in frog node simulations).

The simulated patterns were highly sensitive to variation of the above parameter values. That is, relatively small percentage changes in $\bar{g}_{Na}$ or $\bar{g}_K$ in a bouton produced marked variation in the pattern of simulated currents for that bouton (with lesser changes in the heminode and other boutons). In contrast to this marked sensitivity to perturbations in these variables in the heminode and distal terminal, large alterations in the nodal assignments of $\bar{g}_{Na}$ and $\bar{g}_K$ caused only minor changes in the current patterns. It did not seem reasonable to assign a numerical measure to the degree of correspondence between the simulated and experimental curves because of the considerable variation in the relative sizes of the current peaks observed experimentally from junction to junction. Nevertheless, based on our experience, we determined that it would be difficult to achieve a better overall correspondence, given the constraints on the mechanisms included in the simulation (see Methods: Simulations of presynaptic currents). Table 1 gives the geometrical parameters and channel conductances which were used to generate the curves in Fig. 1*B*.

The ability to simulate membrane currents which match the actual current patterns measured at the nerve ending gave confidence that the corresponding action potentials were also well matched by our simulated action potentials. These action potentials, which were calculated from the parameter set given in Table 1, are shown in Fig. 2; the nerve impulse sweeps over the ending with a very small delay (compared to the duration of the impulse) from the heminode to farthest bouton. However, the amplitude declines as it approaches the distal ends of the terminal where the increased density of K^+ channels causes repolarization to occur earlier.

Delayed-rectifier potassium current in the terminal boutons

This high density of K^+ channels in the terminal branches and boutons, and the corresponding paucity of Na^+ channels, is demonstrated by the application of the potassium channel blocker tetraethylammonium (TEA; Armstrong & Binstock, 1965). Bath application of 10 mM-TEA suppresses the second outward peak in the distal terminal (Fig. 3*A*, top) and the second inward peak in the heminode (Fig. 3*A*, bottom). This shows that a TEA-sensitive, outward K^+ current is generated in the terminal, and that the heminode serves as a passive sink for this current. In addition, it shows that even during blockage of the K^+ conductance with TEA, there is evidence for only a small Na^+ (transient inward) current in the distal terminal.

TABLE 1. Parameters used in the simulation of membrane currents and action potentials in the lizard motor nerve ending.

Feature	Segment no.	Radius μm	Distance μm	$\bar{g}_{Na}$ Siemens	$\bar{g}_{K}$ Siemens
Node 1	0	2·0	2·0	1·200	0·003
	1	2·0	50·0	0·000	0·000
	2	2·0	50·0	0·000	0·000
	3	2·0	50·0	0·000	0·000
	4	2·0	50·0	0·000	0·000
Node 2	5	2·0	2·0	1·200	0·003
	6	2·0	25·0	0·000	0·000
	7	2·0	25·0	0·000	0·000
	8	2·0	25·0	0·000	0·000
	9	2·0	25·0	0·000	0·000
Node 3	10	2·0	2·0	1·200	0·003
	11	2·0	12·5	0·000	0·000
	12	2·0	12·5	0·000	0·000
	13	2·0	12·5	0·000	0·000
	14	2·0	12·5	0·000	0·000
Heminode	15	2·0	4·0	0·600	0·046
	16	1·0	4·0	0·400	0·060
Bouton 1	17	2·5	5·0	0·300	0·171
	18	0·5	2·0	0·240	0·185
Bouton 2	19	2·5	5·0	0·200	0·200
	20	0·5	2·0	0·200	0·218
Bouton 3	21	2·5	5·0	0·200	0·240
	22	0·5	2·0	0·150	0·185
Bouton 4	23	2·5	5·0	0·120	0·150

Each segment was assigned a radius, a longitudinal distance and an Na^+ ($\bar{g}_{Na}$) and K^+ ($\bar{g}_{K}$) channel density. The ending divides into three identical branches at the heminode with each branch containing four boutons and their interconnecting axon segments (see diagram in Fig. 1*B* and text for further details). Computer simulations of membrane currents and action potentials are shown in Figs 1*B* and 2, respectively.

Calcium current

TEA

As in other preparations, blockage of the K^+ conductance with TEA increases the duration of the action potential in the lizard motor nerve several fold (Barrett *et al.* 1988). In addition to blocking the K^+ current, TEA also unmasked a small but prolonged current, which is inward in the terminal boutons (Fig. 3*A*, top) and outward in the heminode (Fig. 3*A*, bottom). During a normal action potential, this current is obscured by the presence of the large K^+ current flowing in the opposite direction; it is revealed when the K^+ current is blocked and the action potential duration is increased several fold.

We determined that this current was carried by calcium ions because: (1) its amplitude was decreased by reducing the bath concentration of calcium (Fig. 3*B*) and (2) it was abolished by substituting cobalt for calcium (data not shown). The observation that this current is inward in the terminal (Fig. 3*A*, top) and is outward in the heminode (Fig. 3*A*, bottom) suggests that the Ca^{2+} channels are sparse (or non-existent) in the heminode but are rich in the terminal branches and boutons. As with

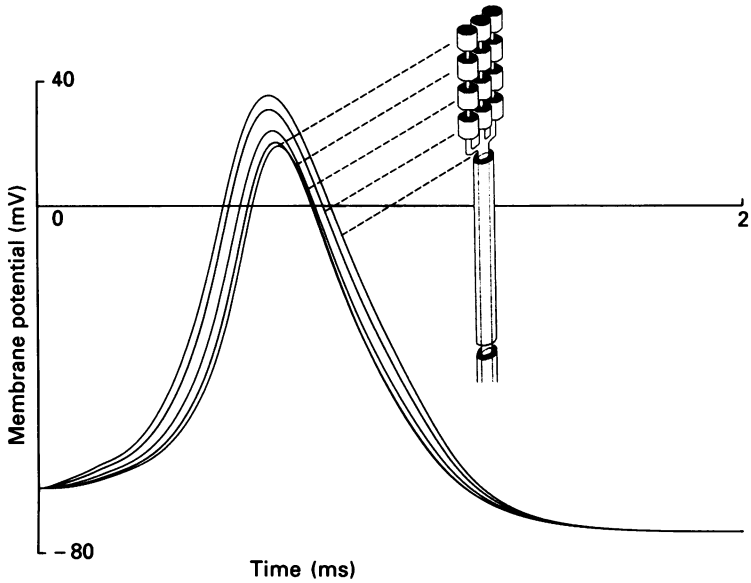

Fig. 2. Simulated action potentials at the heminode and four boutons. Parameters and geometry are the same as those used in Fig. 1*B* (see Table 1).

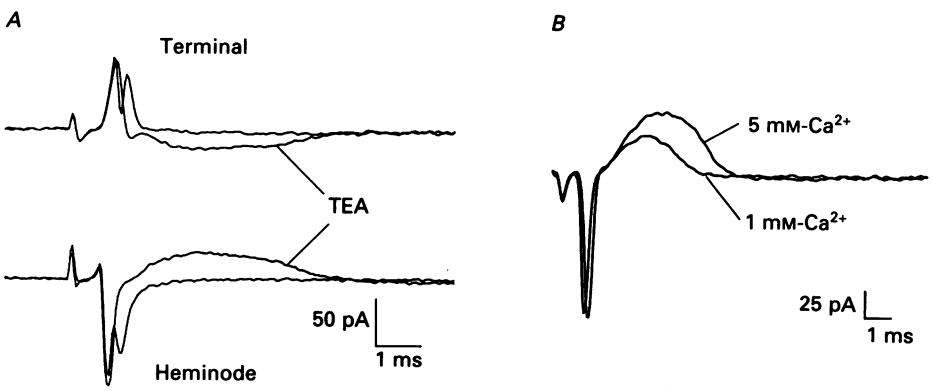

Fig. 3. *A*, calcium current, revealed by blocking the K^+ channels with TEA (10 mM), is inward throughout the terminal (top) but is reflected as outward current in the heminode (bottom). Calcium, 5 mM; pancuronium, 10 μM. Temperature 18 °C. *B*, the reflected Ca^{2+} current, measured in the heminode, is decreased (approximately 40%) by a fivefold reduction in extracellular Ca^{2+}. Temperature 16 °C. Tubocurarine chloride, 100 μM. Each record in panels *A* and *B* is the average of 100 traces obtained at a stimulation rate of 0·5 Hz.

the K^+ current, the heminode again serves as a return path for the calcium current generated in the terminal.

Simulation of K^+ channel block

To simulate the action of TEA, the potassium conductance ($\bar{g}_K$) was set to zero throughout the nerve and nerve ending. Calcium current was added to the simulation

by adding a Ca^{2+} conductance to the terminal branches and boutons. Such a simulation is shown in Fig. 4*A*, where it can be compared with the equivalent experimental traces in Fig. 4*B*. One minor problem was that the action potential did not terminate in the simulation with TEA but stayed up indefinitely. This is because, after the capacitance charging, no net outward current (required for repolarization) developed. In the actual experimental observations (Fig. 4*B*), repolarization may have resulted from an outward current in the nodes or paranodal region. Inclusion of such second order components in our model was deemed unnecessary at this time.

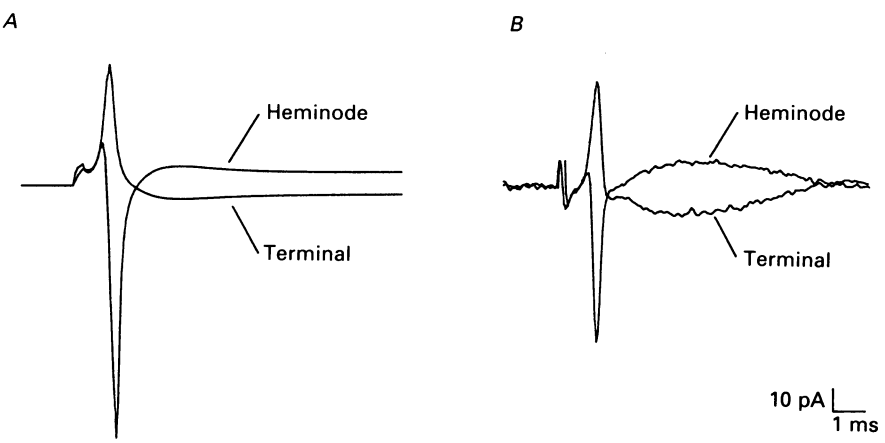

Fig. 4. *A*, simulation of current at the heminode and bouton 2 in the presence of TEA (see Fig. 1*B* for diagram). Parameters and geometry are as described in Table 1, except $\bar{g}_K$ has been set to zero and $\bar{g}_{Ca}$ has been set to 0·25 in segment 17 and to 0·5 in segments 18–23. *B*, experimental current patterns recorded in the presence of 10 mM-TEA at the heminode and distal terminal. Calcium, 5 mM; pancuronium, 10 μM. Temperature 19 °C. Each record is the average of 100 traces (0·5 Hz).

Identification of Ca^{2+} channel type

Neurones express several different types of calcium channel (Miller, 1987). In fact, three types of calcium channel have been shown to *coexist* in several neurones (DuPont, Bossu & Feltz, 1986; Fox *et al.* 1987*a*; Kostyuk, Shuba & Savchenko, 1987). Moreover, in neurones from chick dorsal root ganglia (DRG) three channel types, called L, N and T, can be distinguished on the basis of their sensitivity to pharmacological agonists and antagonists (Fox *et al.* 1987*a*). These results are summarized in Table 2. We measured presynaptic calcium current in lizard nerve endings before and after applying the following inorganic and organic calcium channel blockers: nickel, cadmium, ω-conotoxin GVIA and nifedipine. The results are summarized in Fig. 5. Whereas nickel was ineffective at a concentration of 100 μM (much higher concentrations, e.g. 1 mM, were effective), cadmium blocked the calcium current rapidly and reversibly at only 50 μM (Fig. 5*A*). ω-Conotoxin GVIA, a twenty-seven amino acid peptide component of the venom of the marine snail *Conus geographus* (Olivera, Gray, Zeikus, McIntosh, Varga, Rivier, De Santos &

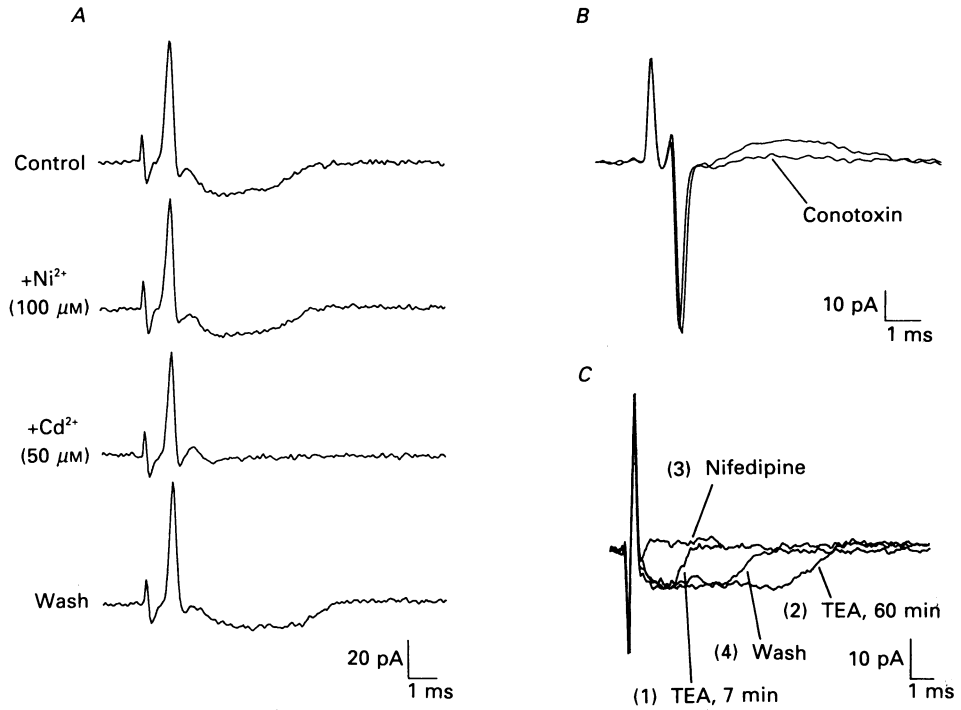

Fig. 5. Pharmacological characterization of calcium current in nerve endings. *A*, calcium current unmasked by addition of 10 mM-TEA (control). Addition of Ni^{2+} to the bathing solution for 15 min caused no change. Following a wash with control saline, Cd^{2+} blocked the Ca^{2+} current immediately (4 min); the block was readily reversed after 8 min in control saline (wash). Calcium, 5 mM; pancuronium, 10 μM. Temperature 18 °C. *B*, superimposed records at the heminode before and after application of 3·5 μM-ω-conotoxin GVIA for 35 min. Calcium, 6 mM; pancuronium, 10 μM. Temperature 20 °C. *C*, superimposed records obtained 7 min after applying 10 mM-TEA (trace (1)); 60 min after applying TEA (trace (2)); 25 min after applying 10 μM-nifedipine in the presence of TEA (trace (3)); and 40 min after washing in control saline (trace (4)). The motor nerve was stimulated as described in the text. Calcium, 3 mM; pancuronium, 10 μM. Temperature 23 °C. Each record in panels *A–C* is the average of 100 traces obtained at a stimulation rate of 0·5 Hz.

Cruz, 1985) also blocked the calcium current but this effect was not reversible with continuous washing (Fig. 5*B*). This is consistent with reports of conotoxin's irreversibility at the frog neuromuscular junction (Kerr & Yoshikami, 1984) and in sensory neurones (McClesky, Fox, Feldman, Cruz, Olivera, Tsien, & Yoshikami, 1987).

Our results with the calcium channel antagonist nifedipine were initially quite variable. Out of six experiments, nifedipine (5–10 μM) reduced the calcium current three times and had no effect in the other three trials. However, nifedipine is reported to require maintained depolarization to block calcium channels in cardiac Purkinje fibres (Sanguinetti & Kass, 1984) and in DRG neurones (Rane, Holz & Dunlap, 1987; Holz, Dunlap & Kream, 1988). Unfortunately, this presents a problem at the neuromuscular junction because measurement of Ca^{2+} current requires that the

nerve impulse propagate into the presynaptic ending. Thus, it is not feasible to maintain the preparation in a chronic depolarized state, such as was possible in the DRG neurones or Purkinje fibres because this would inactivate the Na^+ channels and render the motor nerve inexcitable. Instead, we increased the duration of the action potential several fold and stimulated the nerve repetitively during the application of nifedipine to achieve an effect equivalent to chronic depolarization.

We prolonged the action potential by increasing the amount of time the preparation was exposed to TEA from the normal 5–10 min to at least 1 h. The extent of action potential broadening could be monitored by measuring the duration of the presynaptic current, which provides a good estimate of the length of the action potential. The effect of prolonged exposure to TEA can be seen by comparing trace (1) (Fig. 5*C*), which was measured shortly after applying TEA, with trace (2), which was taken much later. Notice that the amplitude of the Ca^{2+} current is unchanged; only its duration has been affected. This argues that prolonged exposure to TEA has not inactivated a significant fraction of the Ca^{2+} channels, since this would have been observed as a reduction of the total Ca^{2+} current (for example, compare the control traces in panels *B* and *C* of Fig. 12 in Fox *et al.* 1987*a*).

Nifedipine was applied after the action potential duration had been increased to at least 20 ms (trace (2), Fig. 5*C*) and the nerve was given 100 stimuli (at 0·5 Hz) every 5 min. The Ca^{2+} current was progressively reduced until, by 25 min, the current was blocked completely (trace (3)). The nifedipine was then removed, but the stimulation protocol was continued. During this wash-out of nifedipine, the current gradually returned to its control amplitude although it never reached its initial duration. After 40 min of wash the current pattern had stabilized (trace (4)) and additional washing had no further effect. Thus, as with the the DHP sensitivity of high threshold calcium currents in DRG neurones and cardiac muscle cells, the nifedipine-induced inhibition of the calcium current in motor nerve terminals also appears to be voltage and time dependent.

The nifedipine analogue, Bay K 8644, which has been reported to enhance dihydropyridine-sensitive calcium current in DRG neurones (Fox *et al.* 1987*a*; Holz *et al.* 1988), had an erratic effect on the calcium current in our preparation (increase, $n = 2$; decrease, $n = 2$; no effect, $n = 2$).

Relationship of Ca^{2+} current to neurotransmitter release

With the exception of the inconclusive results with Bay K 8644, the pharmacological profile of the Ca^{2+} current observed at the lizard neuromuscular junction is similar to that of the L-type channel described in chick DRG neurones. To determine whether this is also reflected in the ability of Ca^{2+} influx to activate the release of the neurotransmitter acetylcholine (ACh), we tested the sensitivity of neurotransmitter release to the same set of pharmacological agents.

Evoked postsynaptic currents were measured with the same extracellular electrode under conditions of reduced Ca^{2+} (0·25–0·5 mM) and elevated Mg^{2+} (2–8 mM). These conditions were chosen so that we could monitor the amplitude of spontaneous miniature end-plate currents (MEPCs) as well as evoked end-plate currents (EPCs). A change in postsynaptic sensitivity to ACh would be reflected in a change in the average amplitude of the MEPCs. The fact that none of the agents tested altered

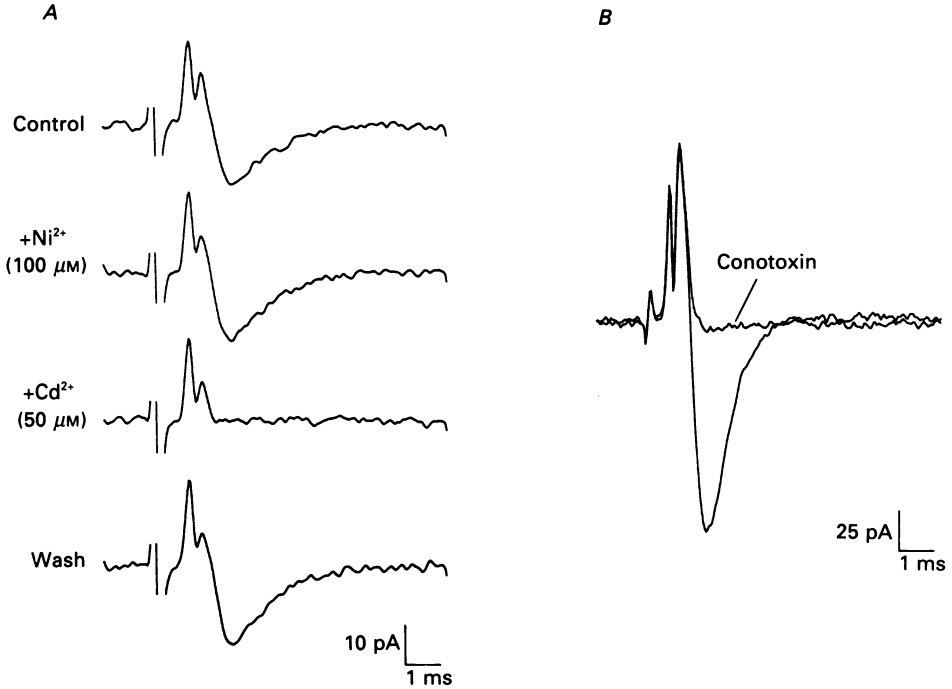

Fig. 6. Pharmacological characterization of transmitter release. *A*, end-plate currents (EPCs) were measured in saline containing 0·5 mM-Ca^{2+} and 4 mM-Mg^{2+} (control). The presynaptic currents (outward) are followed immediately by a large inward current through ACh receptor channels in the postsynaptic membrane. Under these conditions of low quantal release, the EPCs fluctuate in amplitude. The records shown are each averages of 100 traces obtained at a stimulation rate of 0·5 Hz. The preparation was exposed first to 100 μM-Ni^{2+} for 15 min, then washed and exposed to 50 μM-Cd^{2+}, which blocked the EPC immediately (7 min). Washing in control saline for 35 min reversed the effect of Cd^{2+} (wash). Temperature 21 °C. *B*, superimposed averages of forty traces obtained before and after a 26 min application of 5 μM-ω-conotoxin (conotoxin). Stimulation rate, 0·5 Hz. Calcium, 2 mM; tubocurarine chloride, 40 μM. Temperature 20 °C.

MEPC amplitude allowed us to use the EPC amplitude to monitor changes in transmitter release.

Examples of the effects of nickel, cadmium and ω-conotoxin on the EPC are shown in Fig. 6. In normal saline the EPC is a large inward current peaking approximately 1 ms after the first appearance of current at the presynaptic ending. Nickel at 100 μM reduced the EPC only slightly, whereas cadmium at 50 μM abolished it completely (Fig. 6*A*) as did ω-conotoxin at 5 μM (Fig. 6*B*). Thus, these three calcium channel blockers have the same pattern of effects on transmitter release as they had on calcium current.

Nifedipine added to normal saline also inhibited transmitter release. In five out of seven experiments, nifedipine reduced transmitter release (an example is shown in Fig. 7*A*), once it had no effect, and once it actually increased release. As with the experiments on calcium current, endings were treated with TEA or with a combination of TEA and 3,4-diaminopyridine (DAP) to prolong the presynaptic action potential to enhance nifedipine's efficacy. Following pre-treatment with either of these K^+ channel blocking solutions, nifedipine reduced the amplitude of the EPC

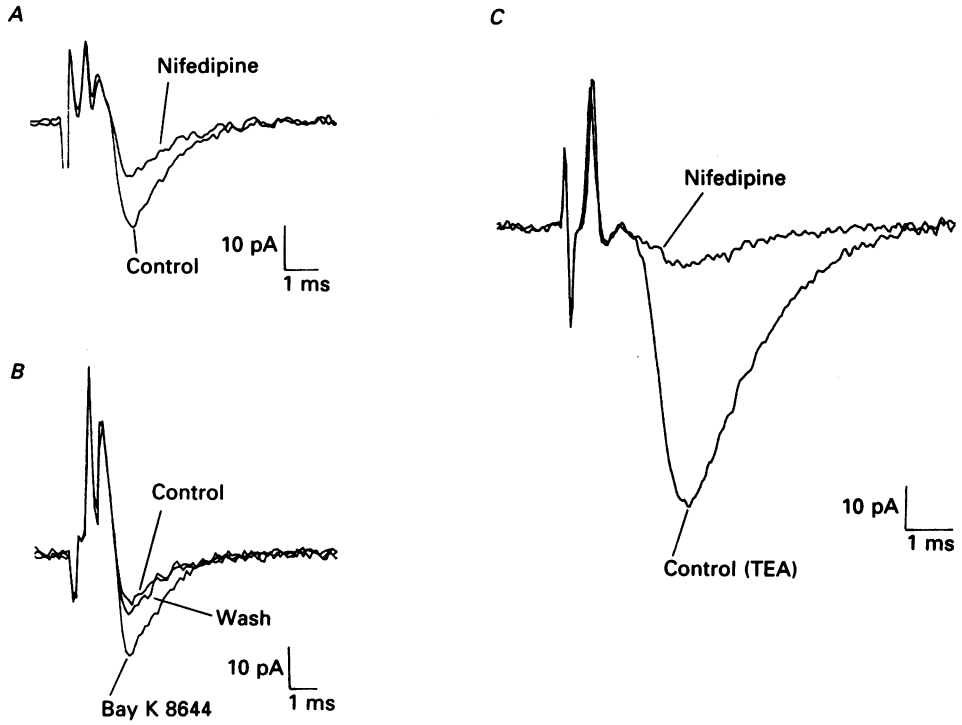

Fig. 7. Sensitivitiy of transmitter release to dihydropyridines. *A*, superimposed records taken before and 11 min after the application of 5 μM-nifedipine. Ca^{2+}, 0·25 mM; Mg^{2+}, 2 mM. Temperature 19 °C. *B*, superimposed records in saline (0·25 mM-Ca^{2+} and 2 mM-Mg^{2+}) before (control), after a 20 min application of 5 μM-Bay K 8644 (Bay K 8644), and then after washing the preparation for 6 min in control saline (wash). The corresponding MEPC frequencies during each of these periods were: control, 1·9 s^{-1}; Bay K 8644, 7·1 s^{-1}; wash, 10·1 s^{-1}. Temperature 23 °C. *C*, superimposed records before and after the application of 10 μM-nifedipine. A preparation was first exposed to 10 mM-TEA for 25 min to increase the duration of the presynaptic action potential (control (TEA)). This produced a very large and prolonged EPC, even though Mg^{2+} was present (5 mM) and Ca^{2+} was reduced to 0·5 mM. Nifedipine was applied and the motor nerve was given 100 stimuli at 0·5 Hz every 5 min. The EPC progressively decreased in amplitude, stabilizing after 30 min at the level shown (nifedipine). This effect was not reversed after 45 min of washing. Each record in panels *A–C* is the average of 100 traces (stimulation rate 0·5 Hz).

by at least 85%. An example of nifedipine's effect following the application of 10 mM-TEA is shown in Fig. 7*C*.

Since, in addition to its effect on presynaptic K^+ channels, TEA also has a postsynaptic blocking effect, MEPCs were reduced in amplitude below the noise level and could not be measured during this latter series of experiments. Thus it was not possible to monitor changes in postsynaptic sensitivity, making it impossible to definitely attribute all of the decrease in postsynaptic current observed in Fig. 7*C* to a decrease in transmitter release *per se*. However, since nifedipine did not alter MEPC amplitude in the experiments performed without TEA (Fig. 7*A*) and recalling that presynaptic calcium current was blocked so convincingly by nifedipine in the presence of TEA (Fig. 5*C*), we are assured that nifedipine's effect on the EPC in Fig. 7*C* results from reduced presynaptic release of neurotransmitter.

Bay K 8644 produced a reproducible and reversible increase in transmitter release

(Fig. 7*B*). In all of seven experiments, Bay K 8644 increased evoked transmitter release by 25–350% (mean = 111%). In contrast to the other calcium channel modifiers used, Bay K 8644 also altered the frequency of MEPCs. In the experiment shown in Fig. 7*B*, Bay K 8644 increased the MEPC frequency from two per minute to approximately ten per minute.

Although evoked release could be restored to control levels within 30 min of returning to control saline, the increase in the spontaneous release of transmitter, induced by Bay K 8644, could not be reversed with washing. Application of Bay K 8644 for 10 min was sufficient to initiate a continuous and rapid increase in the frequency of MEPCs, sometimes to extremely high levels (i.e. > 100 per minute). Atchison & O'Leary (1987) have also reported that Bay K 8644 increases the frequency of miniature end-plate potentials; however, unlike our results, this increase was transient. Since in the present study we were interested primarily in studying evoked transmitter release, we did not pursue further this effect of Bay K 8644 on spontaneous transmitter release. However, our results and those of Atchison & O'Leary (1987) suggest that Bay K 8644 may be having multiple effects at the vertebrate neuromuscular junction.

Calcium-activated potassium current $I_{K(Ca)}$

Another K^+ channel blocker, 3,4-diaminopyridine (DAP), was found to block the delayed-rectifier K^+ channel without affecting the calcium-sensitive K^+ channel, K(Ca). Mallart (1985) reported similar observations at mouse motor nerve endings. As with TEA, DAP unmasked a small inward Ca^{2+} current. However, as shown in traces *B* and *C* in Fig. 8, this inward Ca^{2+} current is followed by a slow outward current which becomes progressively larger over time (5–25 min). This was identified as a calcium-activated K^+ current for the following reasons: (1) it could be blocked by TEA (data not shown), (2) it disappeared when external calcium was replaced by cobalt (trace *D*, Fig. 8), and (3) it was blocked by 50 nM-charybdotoxin (CTX; trace *F*, Fig. 8), a component of scorpion venom and a highly specific blocker of the large, unitary-conductance, calcium-activated potassium channel (Miller, Moczydlowski, Latorre & Phillips, 1985). Anderson, Harvey, Rowan & Strong (1988) reported similar results with CTX at motor nerve endings in the triangularis sterni muscle of the mouse.

When the K(Ca) channel is blocked by CTX an unusual Ca^{2+} current pattern is revealed. In the beginning, the current is constant (as in TEA, see Figs 3–5) but it then grows rapidly to a peak and shuts off abruptly. We interpret the differences in the Ca^{2+} current patterns between those observed with DAP and CTX, and those observed with TEA, to the differences in the way these drugs affect the delayed-rectifier K^+ channel (compare trace *F*, Fig. 8 with Fig. 3*A*). TEA blocks the potassium conductance equally well at all voltages and therefore causes the action potential to develop a prolonged plateau (Hille, 1967). During the plateau the driving force on the Ca^{2+} ions is constant, resulting in a long steady Ca^{2+} current which shuts off quickly at repolarization. In contrast, DAP is less effective in blocking K^+ channels at depolarized potentials (Kirsch & Narahashi, 1978). Therefore, because depolarization relieves the block, DAP causes only a transient

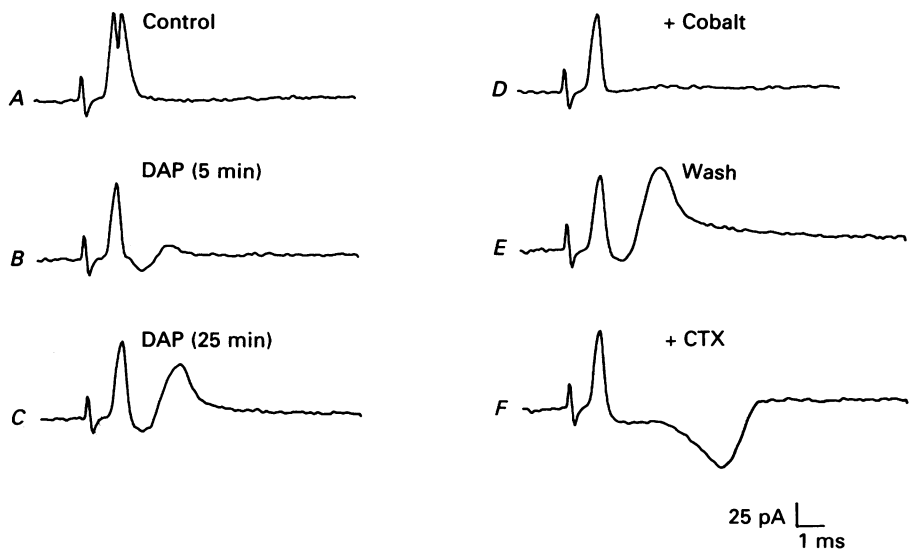

Fig. 8. Calcium-activated K^+current $I_{K(Ca)}$ revealed by 3,4-DAP (0·1 mM) blockage of the delayed-rectifier K^+current. Calcium, 10 mM (except in record *D*, which contained 10 mM-cobalt); pancuronium, 10 μM. Temperature 17 °C. Each record is the average of 100 traces (stimulation rate, 0·5 Hz). *A*, control nerve terminal currents. *B*, after a 5 min application of DAP, a brief inward Ca^{2+} current is revealed, followed by an outward K(Ca) current. *C*, after 25 min in DAP with intermittent stimulation (100 stimuli at 0·5 Hz every 5 min, the K(Ca) current was increased more than fourfold. *D*, substitution of cobalt for calcium abolished both the Ca^{2+} and K(Ca) currents. *E*, both of the currents I_{Ca} and $I_{K(Ca)}$ could be restored promptly upon return of Ca^{2+} to the bath. *F*, addition of charybdotoxin (CTX, 50 nM) abolished the K(Ca) current but not the Ca^{2+} current.

reduction of the K^+ channels. Although prolonged by the DAP, the action potential does not develop a plateau but simply returns slowly to the resting membrane potential. This repolarization increases the driving force on the Ca^{2+} ions and leads to a progressive increase in the Ca^{2+} current, which continues until the Ca^{2+} channels are finally deactivated by the return of the membrane potential to rest.

Relative contribution of K(Ca) current to total outward current

The K(Ca) current above was observed under abnormal conditions; the normal outward K^+ current was blocked, increasing the duration of the action potential, and the Ca^{2+} current was allowed to flow for several milliseconds. Each of these effects would be expected to enhance the K^+ efflux via the K(Ca) channel and distort any picture of its contribution to the time course of a normal action potential. To evaluate its role in repolarization of the nerve terminal membrane under normal conditions, CTX was applied to a preparation in which the normal nerve terminal currents were being recorded, as in Fig. 9. Charybdotoxin slightly delayed and reduced the onset of the outward (K^+) current and prolonged the action potential by about 15% (with no significant effect on the peak amplitude of the outward current). Thus, under normal conditions, the K(Ca) current makes only a small contribution to the repolarization of the terminal membrane.

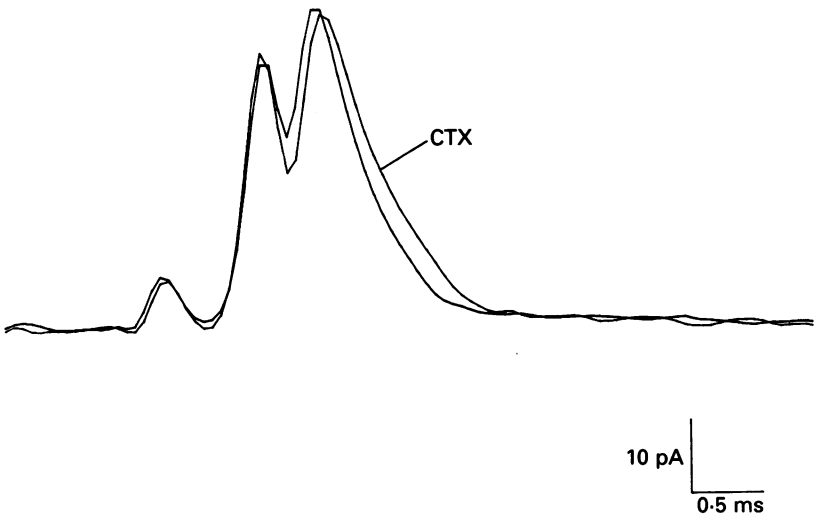

Fig. 9. Charybdotoxin (CTX) blocks part of the terminal K^+current. The control record is the average of seventy-five traces obtained in normal saline with 2 mM-calcium and 11 μM-pancuronium. CTX (25 nM) was added to the saline and 15 min later 100 traces were recorded and averaged (CTX). Temperature 22 °C. Stimulation rate, 0·5 Hz.

DISCUSSION

We have examined the neuromuscular synapse on the ceratomandibularis muscle of the lizard and found that it offers a unique advantage for studying synaptic transmission; the release of neurotransmitter, measured as current in the underlying muscle, can be related directly to the presynaptic currents which activate and regulate its release. These currents, measured from highly localized regions of the presynaptic nerve ending with an extracellular electrode, include Na^+, K^+, Ca^{2+} and K(Ca) currents.

Localization of Na^+ and K^+ channels

The observations of Brigant & Mallart (1982; Mallart, 1985) on the triangularis sterni muscle in the mouse led them to conclude that K^+, Ca^{2+} and K(Ca) channels are present only in the distal region of the nerve endings and that conversely, TTX-sensitive Na^+ channels are present only at the heminode. The latter conclusion has been challenged by Konishi (1985) who detected inward (Na^+) current in the distal terminal after reducing the Na^+ current in the heminode. Furthermore, Peres & Andrietti (1986) were able to qualitatively match the data of Brigant & Mallart even when Na^+ channels were included in the distal regions of the nerve terminal.

We found that in order to match our experimental measurements of presynaptic currents with a computer simulation of membrane currents in the lizard motor nerve ending, it was necessary for Na^+ channels to have a high density in the heminode and K^+ channels to dominate in the terminal boutons. However, we also found that it was

necessary to retain a small Na^+ conductance in the boutons as well as a K^+ conductance in the heminode (see Table 1). Thus, it is our conclusion that whereas Na^+ channels are certainly concentrated in the heminode and K^+ channels in the remainder of the ending, there is some overlap in their distribution.

This arrangement of channels parallels the distribution of Na^+ and K^+ channels in mammalian myelinated nerve fibres. The Na^+ channels are concentrated at the node of Ranvier, analogous to the heminode, and the K^+ channels are restricted to the internodal membrane, analogous to the distal terminal (for a review, see Waxman & Ritchie, 1985). The internodal membrane is normally covered by the myelin sheath, which reduces the electrical load of this region of axon and allows the action potential to propagate through with little attenuation. The nerve terminal, on the other hand, lacks a myelin covering and thus presents a large capacitative load.

Our computer simulations show that if the distance between nodes of Ranvier was 1–2 mm along the entire length of the motor axon all the way down to the nerve ending, then the action potential would not be able to propagate into the terminal; the current generated in the final node would simply not be sufficient to charge the electrical load of the extensive unmyelinated terminal membrane. For the nerve impulse to safely propagate into the terminal, the distance between the nodes of Ranvier must be shortened near the nerve ending. The same conclusion has been drawn by Revenko, Timin & Khodorov (1973) from their simulations of impulse conduction into the motor nerve terminal. Similarly, Waxman & Brill (1978) have shown, in their simulation of the conditions observed in multiple sclerosis, that conduction through demyelinated regions is greatly facilitated by reducing the internodal length near these regions.

Our own observations at the lizard neuromuscular junction and those of Quick *et al.* (1979) at the cat tenuissimus muscle reveal that the internodal spacing does, in fact, gradually decrease from the normal 1–2 mm down to 10–50 μm near the motor nerve ending. Our simulations show that a decreased internodal spacing near the nerve ending allows the impulse to propagate into the terminal without the need for Na^+ channels in the terminal membrane. In fact, the net effect of these short final internodal distances is to make the invasion of the nerve ending so fail-safe that even local application of TTX near the heminode does not block action potential propagation into the terminal (Brigant & Mallart, 1982; Konishi, 1985).

The pharmacological identification and role of the Ca^{2+} channels

The elegant demonstration by Fox *et al.* (1987*a*) that three Ca^{2+} currents in neurones from chick dorsal root ganglia (L, N and T) could be uniquely characterized by their sensitivity to several pharmacological agents has provoked much interest in what type of Ca^{2+} channel is associated with neurotransmitter release (see discussions by Augustine, Charlton & Smith, 1987; Miller, 1987). We think that our observations are the most appropriate for addressing this question because they are the first direct electrical measurements of the effects of several pharmacological agents on Ca^{2+} current and transmitter release at the same synapse. Table 2 presents a comparison of the pharmacological properties of the three Ca^{2+} channel types in DRG neurones with our data at the neuromuscular junction of the lizard. The pharmacological

TABLE 2. Comparison of the pharmacological profiles of T, N and L calcium channels with calcium current and transmitter release

	Chick DRG Neurones			Lizard Neuromuscular Junction	
	T	N	L	I_{Ca}	EPC
Blockers					
Cadmium (50 μM)	No (partial)	Yes	Yes	Yes	Yes
Nickel (100 μM)	Yes	No	No	No	No
ω-Conotoxin	Weak (reversible)	Yes	Yes	Yes	Yes
Nifedipine	No	No	Yes	Yes*	Yes*
Activator					
Bay K 8644	No	No	Yes	—	Yes

T, N and L calcium channels in chick DRG neurones (Fox *et al.* 1987*a*, *b*) compared with calcium current (I_{Ca}) and transmitter release (EPC) at the lizard neuromuscular junction.

* To observe a consistent effect, the preparation was exposed to 10 mM-TEA (see text).

response profile of both Ca^{2+} current and transmitter release at the motor nerve terminal of the lizard match that of the L type channel.

This conclusion is very different from that made at the mouse neuromuscular junction. In the triangularis sterni muscle of the mouse, Anderson & Harvey (1987) failed to observe an effect of ω-conotoxin on extracellular recordings of Ca^{2+} currents and Sano, Enomoto & Maeno (1987) did not see an effect on end-plate potentials. This clearly distinguishes these Ca^{2+} channels from those at both the lizard (reported here) and amphibian neuromuscular junctions (Kerr & Yoshikami, 1984) and from both the N and L type calcium channels in the chick DRG neurones (McClesky *et al.* 1987).

There is general agreement, with the exception of the mouse neuromuscular junction, that transmitter release is not controlled by a T type Ca^{2+} channel, since Cd^{2+} and ω-conotoxin are potent inhibitors of release (see Miller, 1987). There is much disagreement, however, as to whether release is controlled by an N or L type channel. Some studies suggest that transmitter release is controlled by the N type channel because release is totally insensitive to dihydropyridines (Shalaby, Kongsamut, Freedman & Miller, 1984; Kongsamut & Miller, 1986; Hirning, Fox, McCleskey, Olivera, Thayer, Miller, & Tsien, 1988) whereas others suggest the L type channel controls release because transmitter release is inhibited by one or more of the dihydropyridine antagonists (Ogura & Takahashi, 1984; Enyeart, Aizawa & Hinkle, 1985; Turner & Goldin, 1985; Perney, Hirning, Leeman & Miller, 1986; Cazalis, Dayanithi & Nordmann, 1987; Rane *et al.* 1987; Holz *et al.* 1988). There are even a number of studies which implicate both N and L type channels since transmitter release is insensitive to dihydropyridine antagonists but can be activated by the agonist, Bay K 8644 (Middlemiss & Spedding, 1985; Perney *et al.* 1986; Woodward & Leslie, 1986; Atchison & O'Leary, 1987; Loudes, Faivre-Bauman, Patte, & Tixier-Vidal, 1988).

The diversity in these results may reflect a variety of Ca^{2+} channel types present in the preparations studied; however, some of the disagreement may also arise from differences in experimental technique. For example, both we and Holz *et al.* (1988)

found that depolarization was necessary to reveal a consistent block of transmitter release by nifedipine. Thus, the failure to observe an inhibition of transmitter release by nifedipine may not necessarily indicate that N type Ca^{2+} channels control transmitter release, but may instead reflect the voltage dependence of nifedipine's inhibition of L type Ca^{2+} channels (Sanguinetti & Kass, 1984; Fox *et al.* 1987*a*).

Along with membrane voltage, another factor which determines the sensitivity of L type Ca^{2+} channels to dihydropyridines is the level of divalent cations in the extracellular solution. Lee & Tsien (1983) showed that the blocking action of dihydropyridines in heart cells is antagonized by extracellular Ca^{2+}. This may explain why we observed a more consistent effect of nifedipine on transmitter release than on Ca^{2+} current since transmitter release was measured under conditions of reduced Ca^{2+} (0·25–0·5 mM) and Ca^{2+} current was always measured with normal or elevated Ca^{2+} levels (2–6 mM).

Our failure to observe a consistent effect of Bay K 8644 on the Ca^{2+} current in the lizard nerve endings may have resulted from some depolarization of the nerve terminals associated with the application of 10 mM-TEA (which was necessary to reveal the Ca^{2+} current). At depolarized membrane potentials, Bay K 8644 loses its potency as a Ca^{2+} channel agonist, and can even act as an antagonist (Sanguinetti, Krafte & Kass, 1986; Cazalis *et al.* 1987; Fox, Nowycky & Tsien, 1987*b*). Barrett *et al.* (1988) report that 10 mM-TEA depolarizes lizard motor axons by 12–15 mV. This may explain why the effect of Bay K 8644 was erratic during our measurements of Ca^{2+} current but was consistent in increasing evoked neurotransmitter release because the latter measurement did not require TEA application.

Another possible reason for the failure of Bay K 8644 to consistently enhance Ca^{2+} current at the lizard nerve terminal is that the effectiveness of Bay K 8644 is dependent on the frequency of stimulation. Sanguinetti *et al.* (1986) found that Bay K 8644 increases the Ca^{2+} current in heart cells only at frequencies much less than 0·3 Hz (i.e. 0·03 Hz). At a frequency of 0·3 Hz (pulse duration, 50 ms) Bay K 8644 had no effect on Ca^{2+} current and at higher frequencies Bay K 8644 actually decreased Ca^{2+} current! In our experiments the motor nerve was routinely stimulated at 0·5 Hz, which when combined with slightly depolarized nerve terminals, may have prevented the Bay K 8644 from activating Ca^{2+} channels during our direct measurements of Ca^{2+} current. We did not measure the effect of Bay K 8644 on Ca^{2+} current at an appropriately lower stimulus frequency (0·03 Hz) because each measurement of Ca^{2+} current would have taken approximately 1 h to complete (i.e. 100 stimuli at 0·03 Hz). Recording conditions are seldom stable for such a long period of time and any change in the size or shape of the current would have obscured an effect of the Bay K 8644.

The role of the K(Ca) channels

As with Ca^{2+} channels, the K(Ca) channels normally activate too slowly to make a major contribution to the shape of the impulse (see Fig. 9). The role of the K(Ca) channels in the terminal remains to be determined but we suggest two possibilities.

K(Ca) channels may be inserted into the nerve terminal membrane during the fusion of synaptic vesicles with the presynaptic membrane. Several investigators have hypothesized that K(Ca) channels are present in synaptic vesicles and serve to

couple the influx of Ca^{2+} into the presynaptic terminal to the exocytotic release of neurotransmitter (Stanley & Ehrenstein, 1985; Finkelstein, Zimmerberg & Cohen, 1986). This hypothesis predicts that K(Ca) channels should appear in the presynaptic membrane (at least transiently) as a result of the insertion of membrane and integral membrane proteins from synaptic vesicles. Although we have some preliminary data consistent with this hypothesis – the K(Ca) current grows larger with repetitive stimulation (Fig. 8) – we have no direct evidence that synaptic vesicles are the source of K(Ca) channels in lizard motor nerve terminals (see Augustine, Charlton & Horn, 1988 for further discussion of this hypothesis).

K(Ca) channels may be used to speed the repolarization of the terminal region relative to the heminode. Although the heminode and terminal regions are rather tightly coupled in the resting state, the total conductance of the ending increases dramatically during the impulse, decreasing the degree of coupling between the heminode and terminal boutons. In our simulations, the boutons normally repolarize more rapidly than the heminode (see Fig. 2). With the expression of additional outward current from K(Ca) channels, the repolarization could be speeded further. This may be particularly significant when the background intracellular Ca^{2+} level is elevated, such as during a train of impulses; a reduction of the duration of the action potential would restrict the amount of additional Ca^{2+} entry with each impulse.

We are grateful to the National Institutes of Health for financial support in the form of NIH Grant NS03437, to Dr M. L. Hines for the availability of his superb computer program, CABLE; to Mr E. M. Harris for his invaluable technical support and to Mr C. S. Farmer for his help with the preparation of the manuscript. We are further indebted to Drs G. Augustine, M. Charlton, K. Dunlap, A. Fox, M. Nowycky, D. Oertel, R. W. Tsien and J. Zimmerberg for enlightening discussions and comments on the manuscript.

REFERENCES

ANDERSON, A. J. & HARVEY, A. L. (1987). Omega-conotoxin does not block the verapamil-sensitive calcium channels at mouse motor nerve terminals. *Neuroscience Letters* **82**, 177–180.

ANDERSON, A. J., HARVEY, A. L., ROWAN, E. G. & STRONG, P. N. (1988). Effects of charybdotoxin, a blocker of Ca^{2+}-activated K^+ channels, on motor nerve terminals. *British Journal of Pharmacology* **95**, 1329–1335.

ARMSTRONG, C. M. & BINSTOCK, L. (1965). Anomalous rectification in the squid giant axon injected with tetraethylammonium chloride. *Journal of General Physiology* **48**, 859–872.

ATCHISON, W. D. & O'LEARY, S. M. (1987). Bay K 8644 increases release of acetylcholine at the murine neuromuscular junction. *Brain Research* **419**, 315–319.

AUGUSTINE, G. J., CHARLTON, M. P. & HORN, R. (1988). Role of calcium-activated potassium channels in transmitter release at the squid giant synapse. *Journal of Physiology* **398**, 149–164.

AUGUSTINE, G. J., CHARLTON, M. P. & SMITH, S. J. (1987). Calcium action in synaptic transmitter release. *Annual Review of Neuroscience* **10**, 633–693.

BARRETT, E. F. & BARRETT, J. N. (1982). Intracellular recording from vertebrate myelinated axons: mechanism of the depolarizing afterpotential. *Journal of Physiology* **323**, 117–144.

BARRETT, E. F., MORITA, K. & SCAPPATICCI, K. A. (1988). Effects of tetraethylammonium on depolarizing afterpotential and passive properties of lizard myelinated axons. *Journal of Physiology* **402**, 65–78.

BRIGANT, J. L. & MALLART, A. (1982). Presynaptic currents in mouse motor endings. *Journal of Physiology* **333**, 619–636.

CAZALLIS, M., DAYANITHI, G. & NORDMANN, J. J. (1987). Hormone release from isolated nerve endings of the rat neurohypophysis. *Journal of Physiology* **390**, 55–70.

DUPONT, J. L., BOSSU, J. L. & FELTZ, A. (1986). Effect of internal calcium concentration on calcium currents in rat sensory neurones. *Pflügers Archiv* **406**, 433–435.

ELLISMAN, M. H., RASH, J. E., STAEHELIN, L. A. & PORTER, K. R. (1976). Studies of excitable membranes. II. A comparison of specializations at neuromuscular junctions and nonjunctional sarcolemmas of mammalian fast and slow twitch muscle fibers. *Journal of Cell Biology* **68**, 752–774.

ENYEART, J. J., AIZAWA, T. & HINKLE, P. M. (1985). Dihydropyridine Ca^{2+} antagonists: potent inhibitors of secretion from normal and transformed pituitary cells. *American Journal of Physiology* **248**, C510–519.

FINKELSTEIN, A., ZIMMERBERG, J. & COHEN, F. S. (1986). Osmotic swelling of vesicles: Its role in the fusion of vesicles with planar phospholipid bilayer membranes and its possible role in exocytosis. *Annual Review of Physiology* **48**, 163–174.

FOX, A. P., NOWYCKY, M. C. & TSIEN, R. W. (1987*a*). Kinetic and pharmacological properties distinguishing three types of calcium currents in chick sensory neurones. *Journal of Physiology* **394**, 149–172.

FOX, A. P., NOWYCKY, M. C. & TSIEN, R. W. (1987*b*). Single-channel recordings of three types of calcium channels in chick sensory neurones. *Journal of Physiology* **394**, 173–200.

HILLE, B. (1967). The selective inhibition of delayed potassium currents in nerve by tetraethylammonium ion. *Journal of General Physiology* **50**, 1287–1302.

HINES, M. (1989). A program for simulation of nerve equations with branching geometries. *International Journal of Biomedical Computing* (in the Press).

HIRNING, L. D., FOX, A. P., MCCLESKEY, E. W., OLIVERA, B. M., THAYER, S. A., MILLER, R. J., & TSIEN, R. W. (1988). Dominant role of N-type Ca^{2+} channels in evoked release of norepinephrine from sympathetic neurons. *Science* **239**, 57–61.

HODGKIN, A. L. (1937). Evidence for electrical transmission in nerve. Part I. *Journal of Physiology* **90**, 183–210.

HODGKIN, A. L. & HUXLEY, A. F. (1952). A quantitative description of membrane current and its application to conduction and excitation in nerve. *Journal of Physiology* **117**, 500–544.

HOLZ, G. G., DUNLAP, K. & KREAM, R. M. (1988). Characterization of the electrically evoked release of substance P from dorsal root ganglion neurons: methods and dihydropyridine sensitivity. *Journal of Neuroscience* **8**, 463–471.

KATZ, B. & MILEDI, R. (1965). Propagation of electric activity in motor nerve terminals. *Proceedings of the Royal Society* B **161**, 453–482.

KERR, L. M. & YOSHIKAMI, D. (1984). A venom peptide with a novel presynaptic blocking action. *Nature* **308**, 282–284.

KIRSCH, G. E. & NARAHASHI, T. (1978). 3,4-Diaminopyridine: a potent new potassium channel blocker. *Biophysical Journal* **22**, 507–512.

KONGSAMUT, S. & MILLER, R. J. (1986). Nerve growth factor modulates the drug sensitivity of neurotransmitter release from PC-12 cells. *Proceedings of the National Academy of Sciences of the USA* **83**, 2243–2247.

KONISHI, T. (1985). Electrical excitability of motor nerve terminals in the mouse. *Journal of Physiology* **366**, 411–421.

KOSTYUK, P. G., SHUBA, M. F. & SAVCHENKO, A. N. (1987). Three types of calcium channels in the membrane of mouse sensory neurons. *Biological Membranes* **4** 366–373.

LEE, K. S. & TSIEN, R. W. (1983). Mechanism of calcium channel blockade by verapamil, D600, diltiazem and nitrendipine in single dialysed heart cells. *Nature* **302**, 790–794.

LINDGREN, C. A. & MOORE, J. W. (1986). 'Sticky-patch' measurements of currents in nerve terminals of the lizard. *Biological Bulletin* **171**, 495–496.

LINDGREN, C. A. & MOORE, J. W. (1987). Ionic currents at the lizard neuromuscular junction. *Biophysical Journal* **51**, 395a.

LINDGREN, C. A., MOORE, J. W. & SOSTMAN, A. H. (1988). Pharmacological characterization of calcium channels in motor nerve terminals of the lizard. *Journal of General Physiology* **92**, 3a.

LOUDES, C., FAIVRE-BAUMAN, A., PATTE, C. & TIXIER-VIDAL, A. (1988). Involvement of DHP voltage-sensitive calcium channels and protein kinase C in thyroliberin (TRH) release by developing hypothalamic neurons in culture. *Brain Research* **456**, 324–332.

MCCLESKEY, E. W., FOX, A. P., FELDMAN, D. H., CRUZ, L. J., OLIVERA, B. M., TSIEN, R. W. & YOSHIKAMI, D. (1987). Omega-conotoxin: direct and persistant block of specific types of calcium channels in neurons but not muscle. *Proceedings of the National Academy of Sciences of the USA* **84**, 4327–4331.

MALLART, A. (1985). A calcium-activated potassium current in motor nerve terminals of the mouse. *Journal of Physiology* **368**, 577–591.

MIDDLEMISS, D. N. & SPEDDING, M. (1985). A functional correlate for the dihydropyridine binding site in rat brain. *Nature* **314**, 94–96.

MILLER, C., MOCZYDLOWSKI, E., LATORRE, R. & PHILLIPS, M. (1985). Charybdotoxin, a protein inhibitor of single Ca^{2+}-activated K^+ channels from mammalian skeletal muscle. *Nature* **313**, 316–318.

MILLER, F. J. (1987). Multiple calcium channels and neuronal function. *Science* **235**, 46–52.

MOORE, J. W., JOYNER, R. W., BRILL, M. H. & WAXMAN, S. G. (1977). Simulations of conduction in uniform myelinated fibers: relative sensitivity to changes in nodal and internodal parameters. *Biophysical Journal* **21**, 147–160.

OGURA, A. & TAKAHASHI, M. (1984). Differential effect of a dihydropyridine derivative to Ca^{2+} entry pathways in neuronal preparations. *Brain Research* **301**, 323–330.

OLIVERA, B. M., GRAY, W. R., ZEIKUS, R., MCINTOSH, J. M., VARGA, J., RIVIER, J., DE SANTUS, V. & CRUZ, L. (1985). Peptide neurotoxins from fish-hunting cone snails. *Science* **230**, 1338–1343.

PERES, A. & ANDRIETTI, F. (1986). Computer reconstruction of the spread of excitation in nerve terminals with inhomogeneous channel distribution. *European Biophysical Journal* **13**, 235–243.

PERNEY, T. M., HIRNING, L. D., LEEMAN, S. E. & MILLER, R. J. (1986). Multiple calcium channels mediate neurotransmitter release from peripheral neurons. *Proceedings of the National Academy of Sciences of the USA* **83**, 6656–6659.

PROSKE, U. & VAUGHAN, P. (1968). Histological and electrophysiological investigation of lizard skeletal muscle. *Journal of Physiology* **199**, 495– 509.

QUICK, D. C., KENNEDY, W. R. & DONALDSON, L. (1979). Dimensions of myelinated nerve fibers near the motor and sensory terminals in cat tenuissimus muscles. *Neuroscience* **4**, 1089–1096.

RANE, S. G., HOLZ, G. G. & DUNLAP, K. (1987). Dihydropyridine inhibition of neuronal Ca current and substance P release. *Pflügers Archiv* **409**, 361–366.

REVENKO, S. V., TIMIN, YE. N. & KHODOROV, B. I. (1973). Special features of the conduction of nerve impulses from the myelinated part of the axon into the non-myelinated terminal. *Biofizika* **18**, 1074–1078.

SANGUINETTI, M. C. & KASS, R. S. (1984). Voltage-dependent block of calcium channel current in the calf cardiac Purkinje fiber by dihydropyridine calcium channel antagonists. *Circulation Research* **55**, 336–348.

SANGUINETTI, M. C., KRAFTE, D. S. & KASS, R. S. (1986). Voltage-dependent modulation of Ca channel current in heart cells by Bay K 8644. *Journal of General Physiology* **88**, 369–392.

SANO, K., ENOMOTO, K. & MAENO, T. (1987). Effects of synthetic ω-conotoxin, a new type Ca^{2+} antagonist, on frog and mouse neuromuscular transmission. *European Journal of Pharmacology* **141**, 235–241.

SHALABY, I. A., KONGSAMUT, S., FREEDMAN, S. B. & MILLER, R. J. (1984). The effects of dihydropyridines on neurotransmitter release from cultured neuronal cells. *Life Sciences* **35**, 1289–1295.

STANLEY, E. F. & EHRENSTEIN, G. (1985). A model for exocytosis based on the opening of calcium-activated potassium channels in vesicles. *Life Sciences* **37**, 1985–1995.

TURNER, T. J. & GOLDIN, S. M. (1985). Calcium channels in rat brain synaptosomes: identification and pharmacological characterization. *Journal of Neuroscience* **5**, 841–849.

WALROND, J. P. & REESE, T. S. (1985). Structure of axon terminals and active zones at synapses on lizard twitch and tonic muscle fibers. *Journal of Neuroscience* **5**, 1118–1131.

WAXMAN, S. G. & BRILL, M. H. (1978). Conduction through demyelinated plaques in multiple sclerosis: computer simulations of facilitation by short internodes. *Journal of Neurology, Neurosurgery, and Psychiatry* **41**, 408–416.

WAXMAN, S. G. & RITCHIE, J. M. (1985). Organization of ion channels in the myelinated nerve fiber. *Science* **228**, 1502–1507.

WOODWARD, J. J. & LESLIE, S. W. (1986). Bay K 8644 stimulation of calcium entry and endogenous dopamine release in rat striatal synaptosomes antagonized by nimodipine. *Brain Research* **370**, 397–400.